Mechanical Properties of Sintered B_6O-Alkaline Earth Metal Oxide Materials

Enoch N. Ogunmuyiwa*, *Member, IAENG*, Oluwagbenga T. Johnson, *Member, IAENG*, Iakovos Sigalas, and Ayo S. Afolabi, *Member, IAENG*

***Abstract*— Pure B_6O powder and B_6O powders admixed with 1.5 wt% of MgO, 1.4 wt% of CaO, and 0.7 wt% of $CaCO_3$, were sintered and the microstructure, phase composition and mechanical properties were investigated. Pure B_6O powders were sintered at a temperature of 1900ºC and a load of 50 MPa for 20 minutes in an argon environment, while the B_6O-admixed powders were sintered at a temperature of 1850ºC and loads from 50-80 MPa, under the same environment. The addition of the alkaline earth metal oxide additives resulted in the formation of boride and borate phases, depending on the oxide used. More than 96% of theoretical densities were achieved and the result indicates a good combination of hardness (between 31.6–32.1 GPa) and fracture toughness (between 6.1–6.8 MPa.m$^{0.5}$) in the B_6O-alkaline earth oxide materials. The introduction of the additive enhances the improvement in the fracture toughness of the pure B_6O-materials. The fracture mode observed in the sintered materials is mainly transgranular.**

Keywords — Alkaline earth oxide, boron suboxide, fracture toughness, hardness, transgranular.

I. Introduction

AN ideal cutting material combines high hardness with good toughness and chemical stability. In particular hardness and toughness represent opposing properties and there is no single cutting material, which achieves all three conditions simultaneously. Research efforts by material scientists towards the development of materials with a combination of properties approaching or even improving on those of diamond have resulted in considerable results. Boron-rich compounds have proved good candidates for this type of materials. They give rise to a large family of materials with unique crystal structures and a range of interesting physical and chemical properties, which is related to their short interatomic bond lengths due to a strong covalent bonding **[1]**. Boron-rich compound with a structure based on a rigid three-dimensional, α-rhombohedra boron network include boron carbide (B_4C) and boron suboxide (B_6O_{1-x}, nominally B_6O).

B_6O structure (space group $R\bar{3}m$) consists of eight B_{12} icosahedral units situated at the vertexes of a rhombohedra unit cell. The structure can be viewed as a distorted cubic close packing of B_{12} icosahedra units **[2]** connected through oxygen. B_6O has been found to be the third hardest material with hardness for single crystal, of about 45 GPa, closely rivalling that of cubic boron nitride **[3]**. In addition to this hardness, the fracture toughness of this material (B_6O single crystal) was found to be 4.5 MPa.m$^{0.5}$, which approaches that of single crystal diamond at 5 MPa.m$^{0.5}$ and is significantly better than that of single crystal cubic boron nitride (cBN) at 2.8 MPa.m$^{0.5}$ **[4]**. The combination of high hardness, the possibility of cheaper production cost and production without the need for high pressure, unlike diamond and cBN, makes B_6O-based materials a good candidate for cutting tools and other applications where abrasive wear resistance is important.

The development of thermodynamic data for B_6O at high temperatures **[5]** has allowed prediction of the stability and crystalline phases in B_6O materials. This suggests that a careful selection of additives with controlled sintering conditions could result in the production of B_6O materials having unique combination of mechanical properties for industrial applications. Several attempts have been made to improve on the fracture toughness of B_6O through the addition of different materials. B_6O-material made via high-pressure technique with the addition of materials such as diamond, boron carbide and cBN yielded a fracture toughness of 1.8 MPa.m$^{0.5}$ **[6-7]**. The addition of Al_2O_3 has been reported to increase the fracture toughness to a value of 3.1 MPa.m$^{0.5}$ but with a slight reduction in hardness in comparison to pure B_6O material **[8-9]**. The addition of different cobalt containing additives resulted in a fracture toughness of between 3.2–3.9 MPa.m$^{0.5}$ **[10]**. And recently, B_6O materials with different amount of rare-earth oxide additives reported a fracture toughness between 3.9–5.6 MPa.m$^{0.5}$ **[11]**. This paper therefore aims to investigate the densification and mechanical properties of B_6O material sintered with alkaline earth metal oxide additives.

II. Methodology

B_6O powder (3 µm) produced and supplied by IKTS–Dresden, Germany was used for the hot pressing investigations. The powder was charged and milled in an attrition mill using steel balls (2.5 mm diameter) for 20 hours at 400 rpm, with propan-2-ol as a grinding media, to reduce ball wear. The charge to ball ratio was kept at 3:1. The weight of the balls was measured before and after milling to determine weight loss during milling. The mean particle size of the milled powder was 0.5 µm, measured

Manuscript received February 28, 2015; accepted March 10, 2015.

EN Ogunmuyiwa* and AS Afolabi are both with the Department of Civil and Chemical Engineering, University of South Africa, Florida Campus, Johannesburg, South Africa. (*Corresponding author: phone: +27-79-838-1218; e-mail: ogunmen@unisa.ac.za, afolaas@unisa.ac.za).

OT Johnson is with the Department of Mining and Metallurgical Engineering, University of Namibia, Ongwediva Campus, Namibia. (e-mail: ojohnson@unam.na, Johnson.gbenga@gmail.com).

I Sigalas is with the School of Chemical and Metallurgical Engineering, University of the Witwatersrand, Johannesburg, South Africa. (e-mail: iakovos.sigalas@wits.ac.za).

using a Mastersizer 2000 (Malvern Instruments, Germany). The milled B_6O powder was repeatedly washed in 1 M HCl until the liquid colour changed from semi-transparent dirty yellow to colourless with the removal of contaminant from the steel balls, and this was followed by washing in ethanol to remove the remaining H_3BO_3. 0.06 wt% Fe and 0.04 wt% Cr were found as impurities after washing (ICP-OES SPECTRO CIRUS CCD, Spectro-Analytical Instrument (Pty) Ltd, South Africa).

Pure B_6O powders were then mixed separately with 1.5 wt% MgO powder (5 µm, Industrial Analytical), 1.4 wt% CaO powder (5–10 µm, Industrial Analytical) and 0.7 wt% CaCO3 powder (5 µm, Merck South Africa) respectively, these amounts corresponding to a constant value of 1.08 vol% of additives. $CaCO_3$ was additionally used because it is considered more stable than CaO. The mixing was done using a planetary ball mill in methanol for 2 hours at a speed of 200 rpm. After the mixing, the slurry was dried using a rotation evaporator.

Pure B_6O materials were hot pressed (HP20 Thermal Technology) in hBN-lined-graphite dies under argon gas at 1900ºC and a holding pressure of 50 MPa for 20 min, while the powders with additives were sintered at 1850ºC at a pressure of 80 MPa (except for B_6O-MgO material at 50 MPa) and the same isothermal sintering time. The hot pressed samples were 18 mm in diameter and between 3–4 mm in thickness. After sintering the materials were ground to clean their surface from reaction products with the hBN lining. The density of the sintered B_6O samples was determined using Archimedes method and compared with theoretical densities, which were estimated on the basis of the rule of mixture using 2.55 g/cm^3 for B_6O. X-ray diffraction (XRD) for qualitative phase analysis were performed on cross-sections of the sintered materials with a Philips PW1830 using Cu Kα radiation (2θ range: 10–80º; step size 0.028; 40 kV 30mA), and PANanlytical X'Pert HighScore with the ICDD database (release version 2010) for phase identification. Microstructural observations were carried out using scanning electron microscopy (Philips, XL30 SERIES) with attached EDX system.

The Vickers hardness (HV) and fracture toughness (K_{IC}) were measured using indentation techniques under loads of 1 kg (for pure B_6O sample) and 5 kg (for B_6O-alakline earth oxide materials). An average of five measurements was used to determine the properties of the samples, while the K_{IC} was determined via the direct crack measurement method using Anstis's equation **[12]**, (calibration constant, ξ = 0.016; elastic constant, E = 470 GPa **[13]**).

III. Results

Table 1 summarizes the mechanical properties of the sintered materials. The sintered pure B_6O had 96.1% of the theoretical density. The Vickers hardness of this sample was 30.5 GPa measured under 1 kg load. Higher load resulted in material fracturing. Hence, the fracture toughness of this material could not be determined. This agrees with the result presented by other researchers using ultra-high pressures **[6–11]**. Except for the CaO additive, the observed densities for all the B_6O-alkaline earth oxide materials were higher than that of pure B_6O, an indication of good densification.

The Vickers hardness values measured for the B_6O-alkaline earth oxide materials were slightly higher than that of pure B_6O (even for the B_6O-MgO material sintered at the same load, 50 MPa). The alkaline earth oxide additive showed significant increases in the fracture toughness of the produced materials. For example, B_6O-MgO, B_6O-CaO and B_6O-$CaCO_3$ have a Vickers hardness of 31.5, 32.1 and 31.9 GPa respectively, as compared to 30.5 GPa for pure B_6O. The corresponding fracture toughness values measured for these materials ranges between 6.1–6.8 MPa.m$^{0.5}$. In general, for a small addition of the alkaline earth oxide additive there was a significant increase in the fracture toughness compared to pure bulk B_6O, which was found to be brittle.

Table 1 Mechanical properties of produced B_6O powders

	Pure B_6O	B_6O-CaO	B_6O-MgO	B_6O-$CaCO_3$
Applied load (MPa)	50	80	50	80
Measured density (g/cm^3)	2.45	2.44	2.49	2.50
Theoretical density (%)	96.1	94.6	96.5	97.7
Open porosity (%)	0.9	1.45	0.86	0.97
HV (GPa)	30.5±2.1[a]	32.1±1.9[b]	31.6±2.1[b]	31.6±1.7[b]
K_{IC} (MPa.m$^{0.5}$)	Brittle	6.8±1.6	6.1±1.3	6.1±1.7

[a] – represents a load of 1 kg; [b] – represents a load of 5 kg.

XRD phase analysis of the sintered pure B_6O sample and the sintered B6O-alkaline earth oxide materials are shown in Figure 1(a–d). For pure B_6O material **(Figure 1(a))**, only crystalline phases of B_6O were observed. In addition to the B_6O crystalline phases, the sintered B_6O-alkaline earth oxide materials also contains $Mg_2B_2O_5$ peaks in the MgO additive **(Figure 1(b))**; CaB_6 in the CaO additive **(Figure 1(c))**; and B_4C and CaB_6 peaks in the $CaCO_3$ additive **(Figure 1(d))**, respectively. The formation of B_4C could be as a result of carbon pick-up from the graphite dies by diffusion during cooling. This statement was in agreement with the authors in Herrmann et al (2009) **[14]**. The authors reported the formation of borates or borate glasses or oxides for MgO additive and the formation of borides for stable oxide like CaO.

Figure 2 shows the SEM images with EDX of the hot-pressed pure B_6O and B_6O-alkaline earth oxide materials produced. Observations from the micrographs showed that a homogeneous distribution of the secondary (minority) phases was not obtained in these materials; rather there were segregations (pockets) in the microstructure. Pores which could be inherent in these materials due to decomposition reactions at the sintering temperature were seen as dark spots in the samples (at higher magnifications). There were no differences in the distribution of the additives between the centre and the near surface area of the sintered materials. No evidence of any grain growth was observed even at higher magnifications in the sintered materials. The iron pickup in the EDX analysis of the additive-derived materials could have originated from the starting B_6O material. The segregation of the secondary phase in the B_6O-alkaline earth oxide materials **(Figure 2(c & d))** suggests variation in the properties of the materials at different points in the sample.

ISBN: 978-988-14047-0-1
ISSN: 2078-0958 (Print); ISSN: 2078-0966 (Online)

The EDX analysis of all the samples confirmed that the grey phase represents B_6O, while the white represents the boride and borate phases, in agreement with the phase analyses obtained from the XRD analysis. This is in agreement with the authors in **[14–16]**. The non-homogeneous distribution of the secondary phases on these materials could be a result of the poor wettability of the secondary phase with B_6O.

IV. Discussion

A fully densified B_6O compact is difficult to sinter even when applying high pressure sintering techniques such as hot pressing [16], hence the need to develop an appropriate sintering aid is required. This is because B_6O is easily oxidized to form B_2O_3 with the mechanical strength of the resultant sintered compact degraded **[7]**. The degradation of mechanical properties by B_2O_3 has been corroborated by the work done by Andrews, 2008 **[9]**. The presence of B_2O_3 has also shown to lowers the theoretical density of B_6O **[13]**.

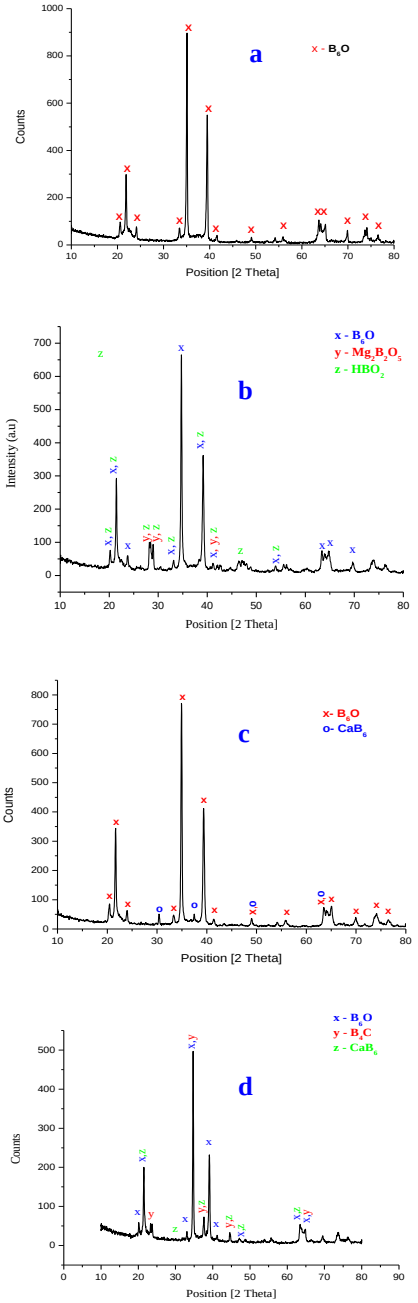

Figure 1 XRD phase analysis of sintered B_6O-alkaline earth metal oxide (a) pure B_6O, (b) B_6O-MgO, (c) B_6O-CaO, and (d) B_6O-$CaCO_3$ materials respectively.

B_6O powders hot pressed either under vacuum or argon conditions at temperatures in the range of 1600°C–1900°C, have produced B_6O materials with densities in the range of 85–97% of the theoretical density **[13,17–20]**. This study produced a density of 2.45 g/cm^3 for pure B_6O, which was about 96.1% of the theoretical density. The difference between the value obtained in this work and others is in the amount of porosity obtained in the sintered material. The presence of the pores has been attributed to the evaporation of B_2O_3 at high temperatures **[14–16]**. It is possible that small amount of B_2O present may have volatilized at high temperatures, partly acts as the source of small pores in the microstructure. As reported by Andrews, 2008 **[9]**, the theoretical density of B_2O_3 is 2.46 g/cm^3, which is less than that of pure B_6O; therefore a small amount of B_2O_3 in the samples will lower the overall theoretical density of a hot pressed B_6O sample.

This work assumed that all the additives in the powder completely transformed to their respective secondary phase(s) after sintering. And also 1 wt. % of B_2O_3 present in the starting material was made in the calculation of theoretical densities. The theoretical densities of the materials were calculated (based on the rule of mixture method) to ascertain the percentage densification obtained by the hot pressing process.

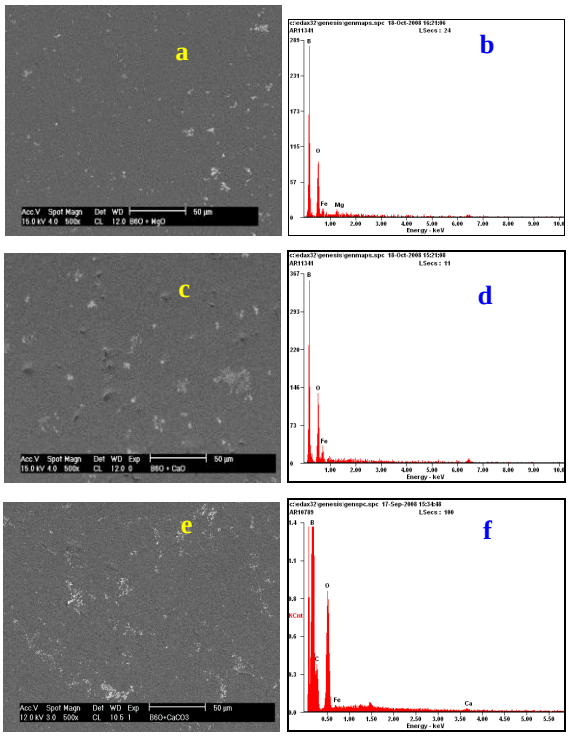

Figure 2 SEM images with EDX analysis of sintered (a & b) B_6O-MgO, (c & d) B_6O-CaO, and (e & f) B_6O-$CaCO_3$ materials.

Sintered B_6O-alkaline earth oxide additives resulted in higher densification as compared with that of pure B_6O (except for B_6O-CaO additive), even when same load was used. XRD patterns of the sintered materials show the

ISBN: 978-988-14047-0-1
ISSN: 2078-0958 (Print); ISSN: 2078-0966 (Online)

formation of a borate phase for MgO additive, a boride secondary phase for CaO additive, and carbide and boride phases for the $CaCO_3$ additive. There are two possible explanations for the improvement in the densities obtained for these materials; one is that the additives form a liquid phase in which B_6O partially dissolves, thus assisting in the densification of the materials at the sintering temperature and recrystallizing during cooling to form the respective secondary phase(s) at the grain boundaries as shown in the XRD patterns. On the other hand, the formation of B_2O_3 as a result of the oxidation reaction occurring in most cases between the B_6O and the sintering additives, suggest that a more liquid phase is formed, thereby improving the densification behavior. Hence, a precise control of the oxygen content would be necessary for the reproducible densification of the materials.

In the B_6O-MgO material **(Figure 2(a))**, segregation of the secondary phase ($Mg_2B_2O_5$) was evident even though there was an increase in the density of the material. Two reasons could be attributed to this: the wettability of the additive with B_6O and the other can be understood from a thermodynamic point of view. To understand and properly explain the densification of this material, there is a need to consider the phase diagram of the MgO-B_2O_3-B_6O system. There is no known phase diagram for this system, but one can consider that of the MgO-B_2O_3 system **(Figure 3)**.

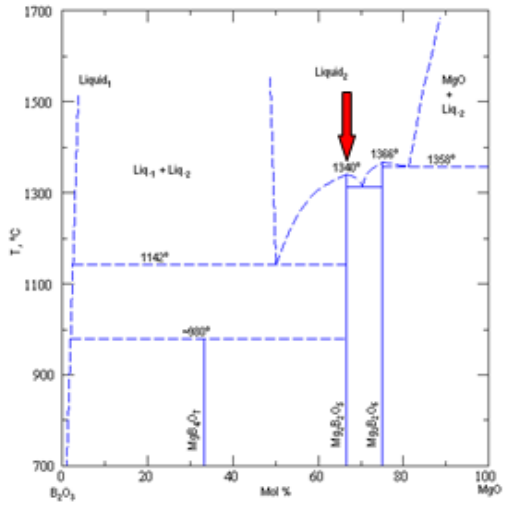

Figure 3 Phase diagram of MgO-B_2O_3 system (ACerS-NIST phase equilibrium diagram, figure 93-028). The arrow indicates the material under consideration **[16]**.

From Figure 3, at the sintering temperature, there is enough liquid present which accelerates mass transport and therefore improves densification. The oxidation reaction between B_2O_3 and MgO resulted in liquid phase formation, which re-crystallized during cooling forming the borate phase ($Mg_2B_2O_5$) at the grain boundaries. Hence, the segregation could be a result of poor wettability of the MgO on B_6O.

For the B_6O-CaO and B_6O-$CaCO_3$ materials **(Figure 2(c & e))**, the segregation of liquid phase in the microstructure might be a result of poor wettability. At the sintering temperature, the existence of B_2O_3 liquid which decomposed leaving pores within the material could be responsible for the decrease densification in the B_6O-CaO material **(Figure 2(c))**. This has a negative influence on the densification and is reflected at the measured porosity value of the material **(Table 1)**. In the case of B_6O-$CaCO_3$ material **(Figure 2(e))**, the improved densification corroborates with the reduced porosity. The reactions for the sintered B_6O-CaO and B_6O-$CaCO_3$ materials can be represented in **equations 1 and 2**.

$$4CaO + 5B_6O \rightarrow 4CaB_6 + 3B_2O_3\uparrow \quad (1)$$

$$4CaCO_3 + 9B_6O \rightarrow 4CaB_6 + 4B_4C + 7B_2O_3\uparrow \quad (2)$$

Figure 4 showed a comparison of sintered pure B_6O material made by other authors. Although the values obtained by some authors **[13,20–21]** seems higher compared to this study, it should be advised however, that the porosity were either not reported or very high. In addition, variations in the sintering conditions (temperature, pressure, time and atmosphere) could affect the amount of porosity present which has a negative effect on hardness. It should however be noted that the hardness value obtained in this study is higher compared to those obtained by Andrews, 2008 **[9]** and Johnson 2008 **[22]**, even at the same load. The hardness values obtained for the sintered B_6O-alkaline-earth metal oxide sintered material were higher than that of the pure B_6O compact. These values obtained show a similar range as seen from the error bars **(Figure 5)**.

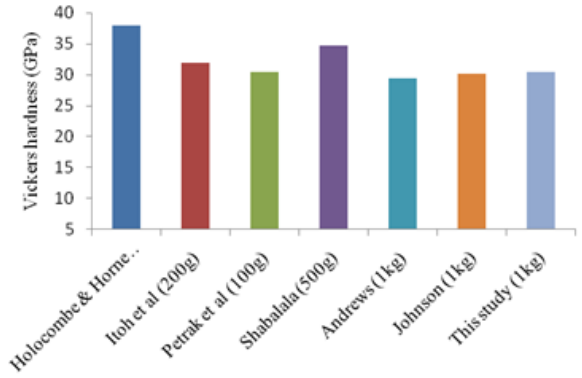

Figure 4 A comparisons of sintered pure B_6O materials made by other authors with this study.

The variation in the hardness values obtained for these materials is also related to the better densifications as compared to the pure B_6O. And although full densification was not achieved in these materials, the average hardness value obtained was encouraging. This suggests that possible improvement in the densification of B_6O material with oxides from this group might result in better hardness values.

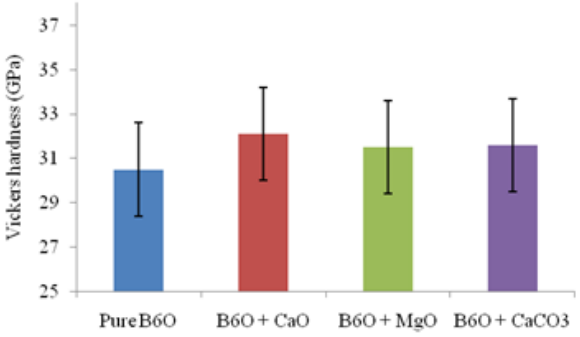

Figure 5 Comparison of the Vickers hardness of the sintered B_6O-alkaline earth metal oxide materials.

ISBN: 978-988-14047-0-1
ISSN: 2078-0958 (Print); ISSN: 2078-0966 (Online)

He et al., 2002 [23], at high pressure between 3–5 GPa made a single crystal of B_6O and recorded a fracture toughness (K_{IC}) of 4.5 MPa.$m^{0.5}$. Pure B_6O sintered compact is generally believed to be brittle and the reason for the very low toughness is not very clear. During the course of hardness measurement on a sintered pure B_6O compact in this study, on increasing the load above 1kg, the material showed a high scattering property with chipping during indentation. It was thus concluded that the material had low K_{IC}. Although it is not clear how fracture occurs in this material, but there were some evidence of transgranular fracture mode. The K_{IC} values of the sintered B_6O-alkaline earth oxide additives reported in this study were measured using a load of 5kg and it ranged between 6.1 and 6.8 MPa.$m^{0.5}$. This showed a significant improvement in the K_{IC} considering the fact that pure sintered B_6O compact is very brittle.

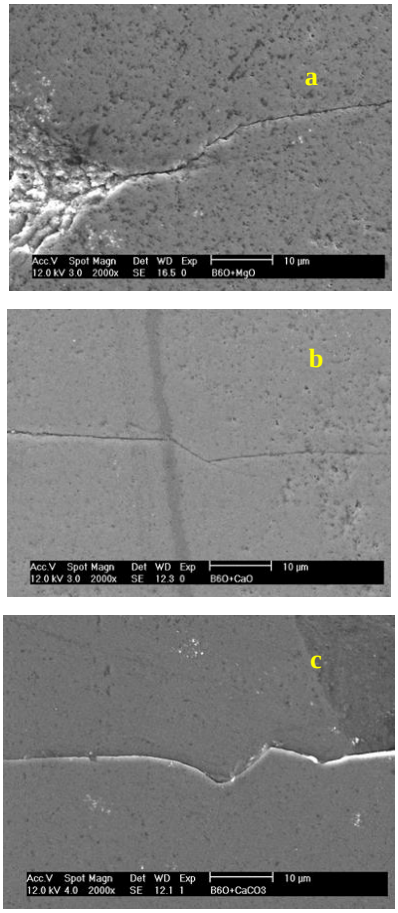

Figure 6 Indentation crack path on sintered (a) B_6O-MgO, (b) B_6O-CaO, and (c) B_6O-$CaCO_3$ materials.

Figure 6(a–c) shows the SEM images of the crack propagation on the polished surfaces of sintered B_6O-alkaline earth oxide materials. Crack propagations on these materials are predominantly transgranular mode and occasions of crack deflection with low deflection angles on the secondary phase (e.g. **Figure 6(e)**). Most of the crack deflections were either caused by the presence of the secondary phase and/or by the inherent pores. These deflections was reportedly caused by non-wetted grain boundary [5,23]. A similar findings was also observed by other authors [15,24]. In comparison to the pure B_6O, the crack path lengths of the B_6O-alkaline earth oxide materials are shorter. The deflection observed can be explained by the stresses that exist in the material. The B_6O matrix has a different thermal expansion coefficient (CTE) compared to the secondary phase(s). This could result in the formation of large internal stress when the material is cooled from the sintering temperature. This difference can induce a tangential compressive stress near the particle/matrix interface and thereby diverts the crack around the particle, making the material tough.

Bush 2011, reported that the effect of the additives on the fracture toughness of B_6O materials is not only dependent on the amount of additive present, as there is no evident relationship between measured fracture toughness and the additive content [25]. This means that the properties of the final phases of the additives have some effect on the fracture toughness of the materials and none of the ceramic toughening mechanisms (crack deflection, internal stresses etc.) can unequivocally explain the increase in the K_{IC} values. Hence, a detailed investigation of fracture behavior is necessary for an understanding and further development of these materials.

V. Conclusions

B_6O admixed with 1.5 wt% of MgO, 1.4 wt% of CaO, and 0.7 wt% of $CaCO_3$, were sintered and the mechanical properties evaluated. The addition of the alkaline earth metal oxide additives resulted in the formation of boride and borate phases, depending on the oxide used. More than 96% of theoretical densities were achieved for these materials. The result indicates a good combination of hardness (between 31.6–32.1 GPa) and fracture toughness (between 6.1–6.8 MPa.$m^{0.5}$) of the B_6O-alkaline earth oxide materials. The investigation indicates that the use of alkaline earth oxides as a sintering aid could be a promising way for the effective and reliable production of B_6O materials with improved hardness and fracture toughness for commercial application. Fracture toughness enhancement could be attributed to the introduction of secondary phases in the B_6O matrix and to bimetallic stresses induced between the matrix and the secondary phase or by many other mechanisms. The investigation showed that the additives used also had the potential of reacting with B_2O_3 present to form other phases that cause bimetallic strain toughening at the grain boundaries. The cracks obtained in these materials showed mainly transgranular fracture mode. Although the fracture mechanism is not completely clear, further work is necessary to understand the mechanism.

Acknowledgement

The authors acknowledge Element Six and National Research Foundation Centre of Excellence in Strong Materials, for financial support.

References

[1] J. Donohue, The structures of the elements, John Wiley, New York, 1974.

[2] M. Kobayashi, I. Higashi, C. Brodhag, and F. Thévenot, Structure of boron suboxide (B_6O) by Rietveld refinement, Journal of Materials Science, 28, (1993) 2129–2134.

ISBN: 978-988-14047-0-1
ISSN: 2078-0958 (Print); ISSN: 2078-0966 (Online)

[3] D. He, Y. Zhoa, L. Daemen, J. Quian, TD. Shen, and TW. Zerda, Boron suboxide: as hard as cubic boron nitride, Applied Physics Letter, 81(4), (2002) 643–645.
[4] CA. Brookes, The mechanical properties of cubic boron nitride – a perspective view, Inst. Phys. Conf. Ser., 75, (1986) 207–220.
[5] HJ. Kleebe, S. Lauterbach, TC. Shabalala, M. Herrmann, and I. Sigalas, B_6O: A correlation between Mechanical Properties and Microstructure Evolution upon Al_2O_3 Addition during hot-pressing, Journal of American Ceramics Society, 91(2), (2008) 569–575.
[6] H. Itoh, I. Maekawa, and H. Iwahara, Microstructure and mechanical properties of B_6O-B_4C sintered materials prepared under high pressure, Journal of Materials Science, 35, (2000) 693–698.
[7] R. Sasai, H. Fukatsu, T. Kojima, and H. Itoh, High pressure consolidation of B_6O-diamond mixtures, Journal of Materials Science, 36, (2001) 5339–5343.
[8] TC. Shabalala, DS. Mclachlan, I. Sigalas, and M. Herrmann, Hard and tough boron suboxide based material, Ceramics International, 34, (2008) 1713–1717.
[9] A. Andrews, M. Herrmann, TC. Shabalala, and I. Sigalas, Liquid phase assisted hot pressing of boron suboxide materials, Journal of European Ceramics Society, 28, (2008) 1613–1621.
[10] OT. Johnson, I. Sigalas, EN. Ogunmuyiwa, HJ. Kleebe, MM Muller, and M. Herrmann, Boron suboxide materials with Co sintering additives, Ceramics International, 36, (2010) 1767–1771.
[11] OT. Johnson, EN. Ogunmuyiwa, I. Sigalas, and M. Herrmann, Boron suboxide materials with rare-earth metal oxide additives, in: Proceedings of International Conference on Manufacturing Engineering and Engineering Management Chemical Engineering and Technology, ICMEEM, World Congress of Engineering, WCE, London, United Kingdom, 3–5 July, 2013, 501 – 505.
[12] GR. Antis, P. Chantikul, BR. Lawn, and DB. Marshall, A critical evaluation of indentation techniques for measuring fracture toughness: I, direct crack measurements, Journal of American Ceramic Society, 64, (1981) 533–538.
[13] TC. Shabalala, The preparation and characterization of boron suboxide (B_6O) based materials, PhD thesis, University of the Witwaterstand, 2007.
[14] M. Herrmann, J. Raethel, K. Sempf, M. Thiele, A. Bales, and I. Sigalas. Field-assisted densification of superhard B_6O material with Y_2O_3/Al_2O_3 addition, Journal of American Ceramic Society, 92, (2009) 2368–2372.
[15] M. Herrmann, I. Sigalas, M. Thiele, MM. Muller, HJ. Kleebe, and A. Michaelis, Boron suboxide ultrahard materials, International Journal of Refractory Metals and Hard Materials, 39, (2013) 53–60.
[16] EN. Ogunmuyiwa, Study of sintering and structure-property relationships in boron suboxide (B_6O)-alkaline earth metal oxide, cobalt, and nickel compound, MSc(Eng) dissertation, University of the Witwatersrand, 2009.
[17] C. Brodhag and F. Thévenot, Hot pressing of boron suboxide $B_{12}O_2$, Journal of Less Common Metals, 117, (1986) 1–6.
[18] IA. Bairamashvili, GI. Kalandadze, AM. Eristavi, JS. Jobava, VV. Chotulidi, and YI. Saloev, An investigation of the physicomechanical properties of B_6O and SiB_4, Journal of Less Common Metals, 67, (1979) 455–561.
[19] IO. Kaylan and OT. Inal, Synthesis of aluminium infiltrated boron suboxide drag cutters and drill bits, Journal of Materials Science, 34, (1999) 4105–4120.
[20] H. Itoh, I. Maekawa, and H. Iwahara, High pressure sintering of B_6O powder and properties of the sintered compact, Journal of the Society of Materials Science, 47, (1998) 1000–1005.
[21] JR. Holcombe, E. Cressie, JR. Horne, and JH. Ottis, Methods for preparing boron suboxide, United State Patent - US 3 660 031.
[22] OT. Johnson, Improvement on the mechanical properties of boron suboxide (B_6O) based materials using other compounds as second phase, MSc(Eng) dissertation, University of the Witwatersrand, 2008.
[23] M. Herrmann, J. Raethel, A. Bales, K. Sempf, I. Sigalas, and M. Hoehn. Liquid phase assisted densification of superhard B6O materials, Journal of the European Ceramic Society, 29, (2009) 2611–2617.
[24] M. Thiele, M. Herrmann, and A. Michaelis. B_6O materials with Al_2O_3/Y_2O_3 densified by FAST/SPS and HIP, Journal of the European Ceramic Society, 33, (2013) 2375–2390.
[25] PR. Bush, On the toughening mechanisms present in boron suboxide materials with sintering aids, MSc(Eng) dissertation, University of the Witwatersrand, 2011.

ISBN: 978-988-14047-0-1
ISSN: 2078-0958 (Print); ISSN: 2078-0966 (Online)